UC Irvine
UC Irvine Previously Published Works

Title

Changes in Membrane Fluidity of the Expanded Mutant Huntingtin Protein with the Phasor-FLIM Approach Signatures of Laurdan

Authors

Benítez-Mata, Balam
Palomba, Francesco
Tan, Zhiqun
et al.

Peer reviewed

Changes in Membrane Fluidity of the Expanded Mutant Huntingtin Protein with the Phasor-FLIM Approach Signatures of Laurdan

Balam Benítez-Mata[1] , Francesco Palomba[1] , Zhiqun Tan[2] ,
Leslie Thompson[3] , and Michelle Digman[1(✉)]

[1] Laboratory for Fluorescence Dynamics, Department of Biomedical Engineering,
University of California, Irvine, CA 92627, USA
`mdigman@uci.edu`
[2] Institute for Memory Impairments and Neurological Disorders,
University of California, Irvine, CA 92627, USA
[3] School of Medicine, University of California, Irvine, CA 92627, USA

Abstract. Huntington's Disease, known for the presence of extended polyQ repeats in the huntingtin protein, has pathological effects on cellular membrane organelles. Here, we describe disturbances in membrane organization caused by the expression of mutant polyQ. We use the environment-sensitive fluorescent probe, LAURDAN, to assess variations in membrane lipid order of SH-SY5Y cells. The cells were induced to express labeled non-pathogenic (Q18mApple) and pathogenic (Q53mApple) proteins. Our approach takes advantage of LAURDAN's affinity for hydrophobic regions, such as membranes, where it displays a red shift in emission associated with higher membrane fluidity (MF) instigated by changes in dipolar relaxation (DR) from the penetration of water molecules into the lipid bilayer. To assess fluidity in membranes, we use the Phasor analysis where we analyze LAURDAN fluorescence lifetime. In the phasor analysis plot, we identify two axes, one sensitive to MF and another to DR. Here we show that expression of pathogenic polyQ, correlates with increasing membrane fluidity, with no changes in DR processes, that suggests a disturbance in water penetration but not in membrane-lipid composition. Moreover, we show MF and DR processes are not inversely proportional and can be distinguished apart using lifetime measurements.

Keywords: Fluorescence microscopy · Membrane fluidity · Huntington's Disease

1 Introduction

Huntington's disease (HD) is a neurodegenerative disease characterized by the expression of abnormal poly-glutamine (CAG) repeats (polyQ) in the huntingtin (Htt) protein. Expanded polyQ longer than 35 polyQ repeats in the exon 1 of the huntingtin gene,

are considered pathogenic (mHtt). These extended polyQ repeats dysregulate the native protein function by assembling into aggregates and forming inclusions [1]–[3]. HD affects cholesterol metabolism by dysregulating the transcription of PGC1α, SREBP and LXR, altering biosynthesis and lowering intracellular levels of cholesterol, leading to membranes deterioration, and compromising cellular organelles now prone to dysfunctionality [4].

In Huntington's disease there are disturbances in lipids composition that impact membrane fluidity (MF) or water penetration into the membrane bilayer. These types of lipids include but are not limited to cholesterol, GM1 gangliosides, monounsaturated and polyunsaturated fatty acids docosahexaenoic acid (DHA) and arachidonic acid (AA) [5]–[8]. Our work as well as others, have shown that overall, MF increases in mHtt cells [9, 10]. However, membrane fluidity is not only lipid dependent, proteins within the membrane bilayer also have effects in it [11].

Here we use LAURDAN as a membrane order reporter, a probe with relative high quantum yield, photostability and with negligible cytotoxicity. LAURDAN shows a red-spectral shift as the membrane environment polarity increases, providing information about MF and Dipolar Relaxation (DR) (Fig. 1A). Fluorescence lifetime imaging microscopy (FLIM) measures the average time electrons remain in an excited state before decaying back to ground state. The phasor approach enables the graphical representation of lifetimes on a polar coordinate system [12, 13]. Golfetto et al. used the phasor approach to FLIM to describe the sensitivity of LAURDAN lifetime to separately detect MF and DR, which are thought to be inversely proportional, the latter one reports on the mobility of hydrated lipid moieties, either saturated or unsaturated, where the LAURDAN molecule is inserted [14]–[16]. To the best of our knowledge, there are no reports showing how mHtt affects DR in all cell membranes (total membranes).

Here we use LAURDAN lifetime to investigate the MF and DR processes in total membranes during the expression of mHtt polyQ53. We quantify MF and DR changes using a three-component analysis and the Phasor approach to lifetime measurements. We hypothesize this approach can distinguish between changes in MF and DR processes in total membranes as a consequence of mHtt disturbing lipids metabolism.

2 Methods

2.1 Materials

Chemicals used: LAURDAN in crystal-powder form (6-dodecanoyl-2-dimethylaminonaphthalene), Thermo-Fisher Scientific Inc., Ponasterone-A Santa Cruz Biotechnology, Inc., Cell culture reagents from Genesee Scientific Corporation., Antibiotic cocktail made of Zeocin, Invitrogen, and Geneticin, GIBCO.

2.2 Cell Culture

We cultured human derived neuroblastoma SH-SY5Y cell, a widely used model in neurodegenerative diseases. Stable cell lines were generated to respond to ponasterone induction such that this inducible system allows for the expression of the expanded

Exon 1 (Httex1) containing either 18Q or the pathogenic 53Q repeats followed by the fluorescent tag protein mApple, or just mApple as control. The cells are maintained in DMEM/F12 1:1 medium, supplemented with 120 µg/mL of the antibiotic cocktail and 10% FBS. Cells are passaged every 2–3 days. For experiments, cells are plated 48 h prior to imaging in 8-chambered cover glass dishes (Cellvis). Cells are left to adjust overnight followed by Ponasterone induction, 10 µM, for 24 h to express the fluorescent constructs. Cells are washed with complete medium, stained and incubated with a final concentration of 6 µM LAURDAN dissolved in DMSO (final concentration < 0.2% v/v) for 60 min. Cholesterol depletion experiments, are done with MβCD, diluted in deionized water, final concentration 10 µM.

2.3 Fluorescence Lifetime Imaging Microscopy

FLIM acquisition is carried out as previously reported [17]. Briefly, a Zeiss LSM880 coupled to a 2-photon laser (80 fs ultra-short pulse width with an 80 MHz repetition rate) set at 780 nm. A Plan-Apochromat 63x oil immersion objective NA 1.4 (Carl Zeiss). Detection by two high efficiency GaAsP Hybrid Detectors (HPM-100-40, Becker and Hickl GmbH). LAURDAN fluorescence is split with a 495 nm LP dichroic and into two bandpass filters (Semrock) centered at 460/80 nm for Channel 1 and 540/50 nm for Channel 2. Acquisition parameters: frame size is 256 × 256 pixels, pixel dwell time is 16.38 µs/pixel, pixel size is 264 nm. The fluorescence lifetime decays are recorded and calibrated with SimFCS v4 software, available from the Laboratory for Fluorescence Dynamics (www.lfd.uci.edu). For the phasor analysis, a median filter (3 × 3) is applied to all phasor plots using the SimFCS software.

2.4 The Phasor Approach for Lifetime Data

The phasor approach relies on the fluorescence time decay at each pixel in an intensity image, this fluorescence decay consists of different photon arrival times to the detectors, emitted upon the fluorophore excitation. The phasor analysis uses a Fourier transformation applied to each pixel of the image to obtain the $G_{(\tau)}$ and $S_{(\tau)}$ coordinates, corresponding to the x- and y-coordinates in a scatterplot, respectively, using Eqs. 1 and 2. Each pixel in the image is now referred as a phasor, plotted in a polar plot, also denominated as the Phasor plot (Fig. 1B).

$$G_{(\tau)} = \frac{\int_0^\infty I_{i,j}(t)cos(\omega t)dt}{\int_0^\infty I_{i,j}(t)dt} \tag{1}$$

$$S_{(\tau)} = \frac{\int_0^\infty I_{i,j}(t)sin(\omega t)dt}{\int_0^\infty I_{i,j}(t)dt} \tag{2}$$

where $I_{i,j}(t)$ indicates the recorded intensity in pixel (i,j) at time t, f is the laser repetition frequency, used to obtain the angular modulation frequency, $\omega = 2\pi f$. The Phasor plot is a semi-circle, where mono-exponential lifetime decays will lie along the line. Multi-exponential decays will be plotted inside the semi-circle.
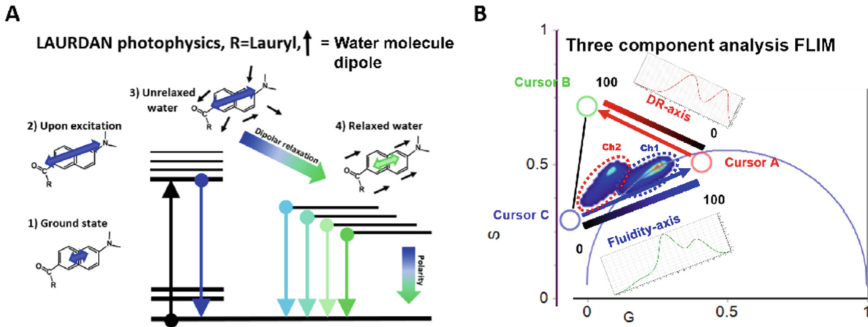
Fig. 1. A) Photophysics of LAURDAN. B) The phasor plot and the three-component analysis of phasor distributions of LAURDAN lifetimes for detection channels 1 and 2, blue and red, respectively.

2.5 Phasor Distributions Analyzed by the Three-Cursor Approach

The three-component analysis is a way to quantify the contribution of three independent components to a single pixel making use of the addition rules that apply to phasor plots. For this work, three cursors are set based on LAURDAN's global lifetime changes in both Channel 1 and Channel 2 combined, to quantify MF and DR (Fig. 1B). The line from cursors "A" to "C", represent the changes referring to MF. A characteristic shift of the phasors position from longer (0,0) to shorter (1,0) lifetimes is related to a shift from nonpolar region (high cholesterol) to polar region (low cholesterol) [16, 17]. To detect DR on LAURDAN's lifetime, a third cursor, "B", is placed outside the universal circle, creating the line A-B. The analysis allows the obtention of histograms with the fraction for MF and DR (Fig. 1B).

$$\text{Fluidity fraction} = \frac{f_c}{f_c + f_a} \tag{3}$$

$$\text{Dipolar relaxation fraction} = \frac{b}{f_b + f_a} \tag{4}$$

For every fractional distribution in each axis, the center of mass (CM) is calculated as:

$$\text{centre of mass(CM)} \frac{\sum_{i=0}^{i=100} F_i * i}{\sum_{i=0}^{i=100} F_i} \tag{5}$$

where F_i represents the fraction corresponding to each axis, either MF or DR.

2.6 Statistics

GraphPad Software, Inc. is used to analyze three independent biological replicates with 10 cells each. For MβCD treatments only one replicate with 10 cells each, is used. Fractional histograms show the mean and positive standard deviation (SD). Violin plots are shown as median with minimum and maximum values. For multiple groups comparison an ANOVA with Tukey post-test is performed. For statistical significance, a p-value lower to 0.05 is used.

3   Results

3.1   Expression of mHtt with a PolyQ53 Increases Membrane Fluidity in Total Membranes

The lifetime phasor plot for LAURDAN's channel 1 emission in SH-SY5Y cells expressing the different Htt constructs is shown in Fig. 2. The phasor distribution is analyzed with the three-component analysis to assess changes in the fluidity and DR axes (Fig. 2A). For each axis, a fractional histogram ranging from 0 to 100 is used for easier interpretation of data. An increase in fraction, represents an increase in each axis. A color scale map is used to visualize lifetime changes of LAURDAN in each condition, along with an intensity-based image of the fluorescently tagged construct (Fig. 2B).
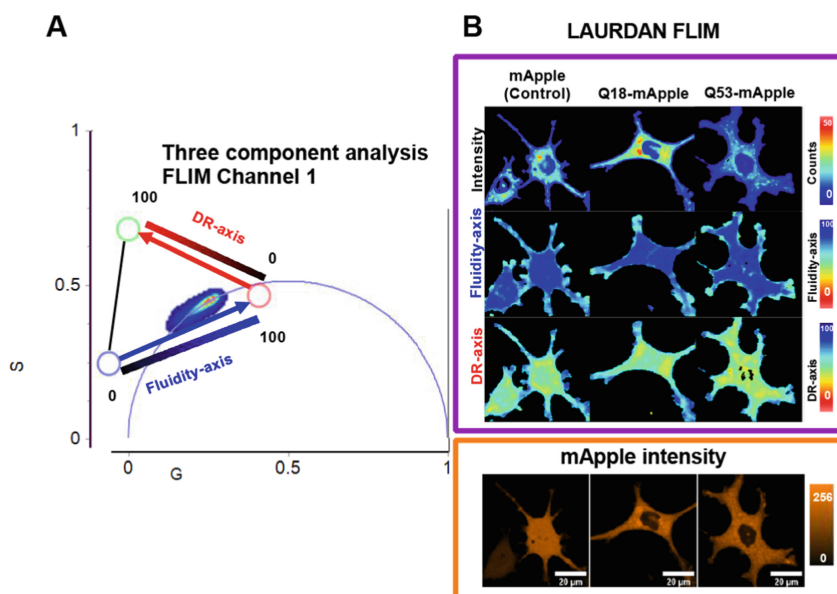

Fig. 2. Analysis on Channel 1, sensitive to polarity. A) Example of Phasor plot distribution for mApple and polyQ constructs. A three-component analysis is shown for MF and DR axes. B) Exemplary images of LAURDAN's intensity emission and pseudo colored lifetime values for Fluidity and DR.

Expression of polyQ53 increases the fluidity fraction in total membranes when compared against a nonpathogenic polyQ18 and mApple constructs (Fig. 3A). This aligns with an increase in the CM of the fluidity-axis (Fig. 4A). This effect has been previously reported by our group using hyperspectral phasors in a PC12 cell model that expresses a polyQ97-mRuby [9].

When cholesterol is depleted with MβCD for all conditions, the MF increases as previously reported [9, 16]. Worth to mention that the polyQ53 + MβCD condition, although not statistically different from MβCD controls, presents a narrower distribution of CM values, this may be an indicative of a more efficient depletion of lipids in the cells expressing the mutant polyQ53.

The DR-axis in channel 1 is virtually not sensitive to DR processes, and variations correspond to the spectral red-shift within channel 1 detection's bandwidth, which lies within the line of the universal circle in the phasor plot (Fig. 2A).
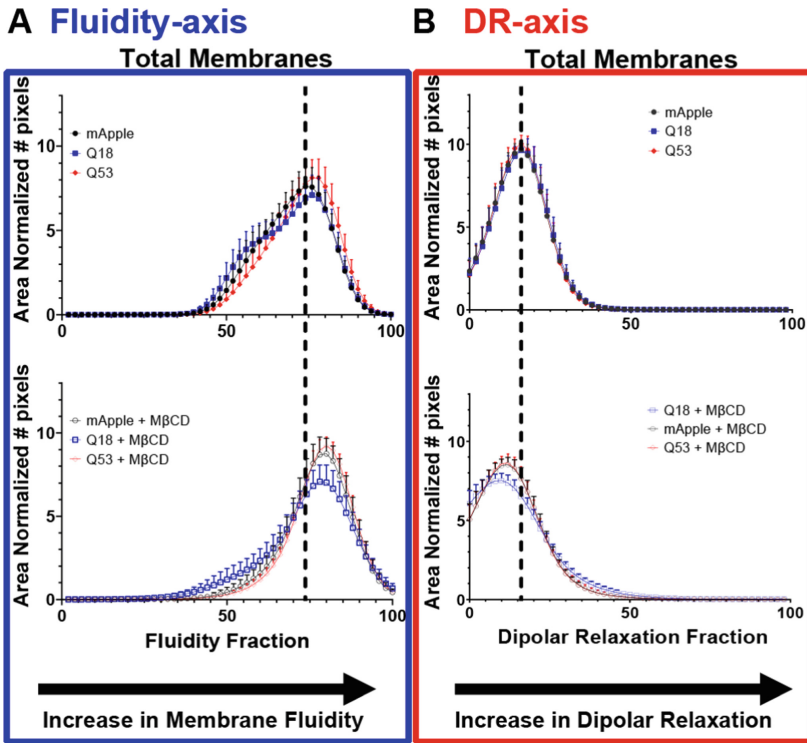
Fig. 3. Analysis on Channel 1, for each cell a A) Fluidity fraction, top, and B) Dipolar Relaxation Fraction, bottom, histograms are created. We show the average and standard deviations (mean + SD). Negative SD is avoided for simplicity.
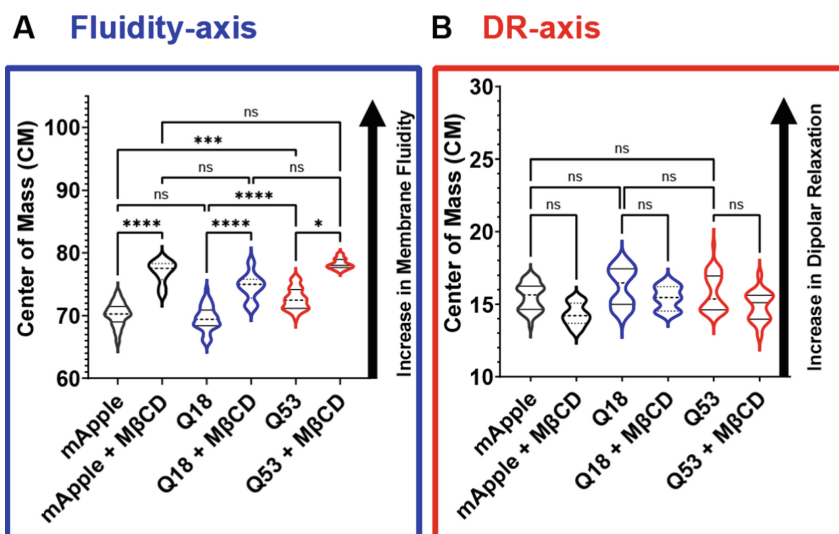
Fig. 4. Analysis on Channel 1, from each individual histogram in Fig. 3, a Center of Mass for A) Fluidity- and B) DR-axes are calculated. Statistical significance is designated with ****, ***, ** and *. Where $p < 0.0001$, $p < 0.001$, $p < 0.01$ or $p < 0.05$, respectively.

3.2 Expression of mHtt PolyQ53 Does not Increases DR Processes in Total Membranes

Channel 2 is sensitive to MF changes due to the spectral shift, but also has sensitivity to DR processes caused by the types of lipids present in the membrane, which causes a rotation of the phase angle and locates the phasors outside of the universal circle with respect to channel 1 due an apparent time delay of emitted photons with respect to excitation (Fig. 1) [16]. Figure 5 shows the three-component analysis done for channel 2 the same way as done for Channel 1.
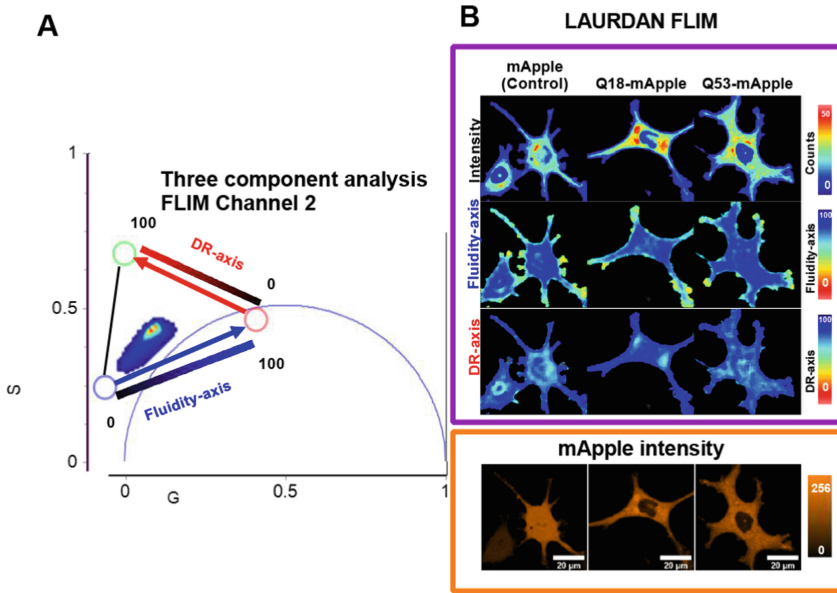
Fig. 5. Analysis on Channel 2 sensitive to DR. A) Example of Phasor plot distribution for mApple and polyQ constructs. A three-component analysis is shown for MF and DR axes. B) Exemplary images of LAURDAN's intensity emission and pseudo colored lifetime values for Fluidity and DR.

Changes in the fluidity-axis detected in Channel 2 suggest an amplified effect on MF caused by polyQ53 (Fig. 6A and Fig. 7A).

We do not observe a significant difference in DR processes between cells expressing pathogenic and control constructs. Changes in DR are thought to be inversely proportional to MF effects, phenomenon shown in samples treated with MβCD for cholesterol depletion, where MF increases and DR decreases (Fig. 6 and Fig. 7).

However, expression of polyQ53 might be affecting the lipids packaging (hydration level) but not their moieties' dynamics, since DR mainly reports the mobility of hydrated lipid moieties, dependent on the type of lipid, saturated or unsaturated, where the LAURDAN molecule is inserted [14, 15].
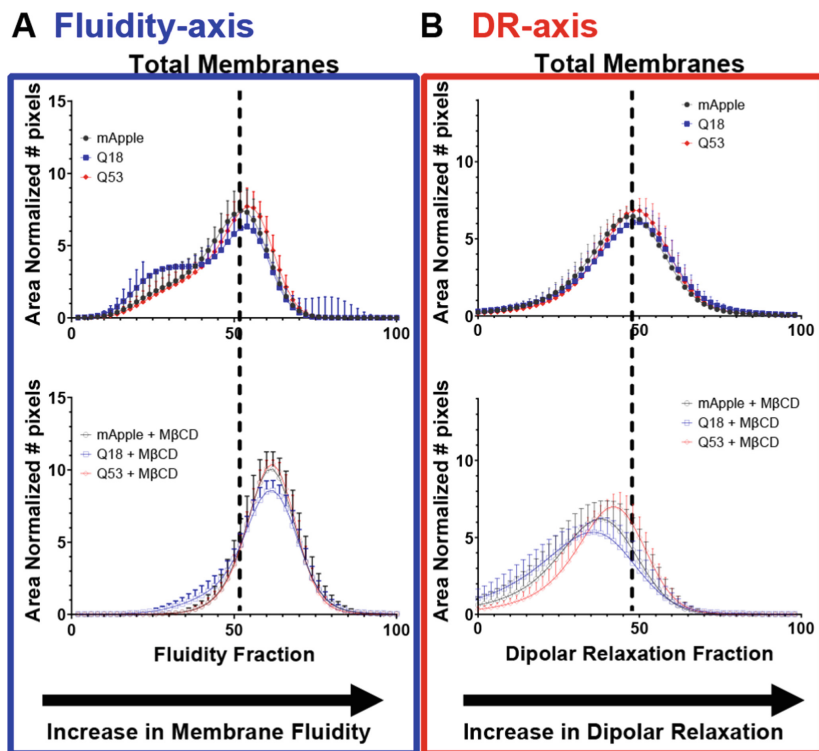
Fig. 6. Analysis on Channel 2, for each cell a A) Fluidity fraction, top, and B) Dipolar Relaxation Fraction, bottom, histograms are created. We show the average and standard deviations (mean + SD). Negative SD is avoided for simplicity.
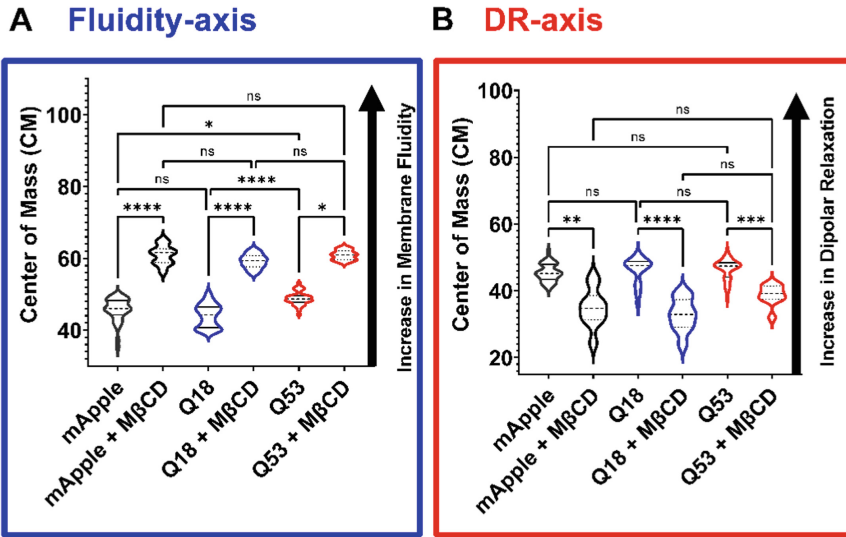
Fig. 7. Analysis on Channel 2, from each individual histogram in Fig. 3, a Center of Mass for A) Fluidity- and B) DR-axes are calculated. Statistical significance is designated with ****, ***, ** and *. Where p < 0.0001, p < 0.001, p < 0.01 or p < 0.05, respectively.

4   Conclusion

Our results indicate that in the absence of inclusions of mHtt polyQ53, there is an increase in membrane fluidity but no changes in DR. This opens a new discussion threat where LAURDAN photophysic-properties report on MF and DR are not inversely proportional processes and can be isolated by measuring the probe's lifetime. Further studies in lipid composition of membranes are needed to confirm this result.

To our knowledge, this is the first time the phasor approach is used for LAURDAN lifetime measurements, which enables the study and isolation of MF and DR processes in an HD cell model.

In this work, we show that expressing the expanded mHtt polyQ53 in HD-SH-SY5Y cells, increases the membrane fluidity without further sign of decrease in DR processes, suggesting disturbances in membrane hydration levels but not in lipid packaging and dynamics of their moieties, in the absence of mHtt inclusions.

References

1. Testa, C.M., Jankovic, J.: Huntington disease: a quarter century of progress since the gene discovery. J. Neurol. Sci. **396**, 52–68 (2019). https://doi.org/10.1016/j.jns.2018.09.022

2. Kim, Y.E., et al.: Soluble oligomers of PolyQ-expanded huntingtin target a multiplicity of key cellular factors. Mol. Cell **63**(6), 951–964 (2016). https://doi.org/10.1016/j.molcel.2016.07.022

3. Kremer, B., et al.: A worldwide study of the Huntington's disease mutation: the sensitivity and specificity of measuring CAG repeats. N. Engl. J. Med. **330**(20), 1401–1406 (1994). https://doi.org/10.1056/NEJM199405193302001

4. Leoni, V., Caccia, C.: The impairment of cholesterol metabolism in Huntington disease. Biochim. Biophys. Acta - Mol. Cell Biol. Lipids **1851**(8), 1095–1105 (2015). https://doi.org/10.1016/j.bbalip.2014.12.018

5. Gaus, K., Zech, T., Harder, T.: Visualizing membrane microdomains by Laurdan 2-photon microscopy (Review). Mol. Membr. Biol. **23**(1), 41–48 (2006). https://doi.org/10.1080/09687860500466857

6. Alpaugh, M., et al.: Disease-modifying effects of ganglioside GM1 in Huntington's disease models. EMBO Mol. Med. **9**(11), 1537–1557 (2017). https://doi.org/10.15252/emmm.201707763

7. Mesa-Herrera, F., Taoro-González, L., Valdés-Baizabal, C., Diaz, M., Marín, R.: Lipid and lipid raft alteration in aging and neurodegenerative diseases: a window for the development of new biomarkers. Int. J. Mol. Sci. **20**(1), 5 (2019). https://doi.org/10.3390/ijms20153810

8. Sambra, V., Echeverria, F., Valenzuela, A., Chouinard-Watkins, R., Valenzuela, R.: Docosahexaenoic and arachidonic acids as neuroprotective nutrients throughout the life cycle. Nutrients **13**(3), 986 (2021). https://doi.org/10.3390/nu13030986

9. Sameni, S., Malacrida, L., Tan, Z., Digman, M.A.: Alteration in fluidity of cell plasma membrane in huntington disease revealed by spectral phasor analysis. Sci. Rep. **8**(1), 1 (2018). https://doi.org/10.1038/s41598-018-19160-0

10. Subczynski, W.K., Pasenkiewicz-Gierula, M., Widomska, J., Mainali, L., Raguz, M.: High cholesterol/low cholesterol: effects in biological membranes: a review. Cell Biochem. Biophys. **75**(3–4), 369–385 (2017). https://doi.org/10.1007/s12013-017-0792-7

11. Lenaz, G., Castelli, G.P.: Membrane fluidity: molecular basis and physiological significance. In: Structure and Properties of Cell Membrane: Volume I: A Survey of Molecular Aspects of Membrane Structure and Function, vol. I, pp. 93–136. CRC Press (1985)

12. Digman, M.A., Caiolfa, V.R., Zamai, M., Gratton, E.: The phasor approach to fluorescence lifetime imaging analysis. Biophys. J. **94**(2), L14–L16 (2008). https://doi.org/10.1529/biophysj.107.120154

13. Ranjit, S., Malacrida, L., Jameson, D.M., Gratton, E.: Fit-free analysis of fluorescence lifetime imaging data using the phasor approach. Nat. Protoc. **13**(9), 1979–2004 (2018). https://doi.org/10.1038/s41596-018-0026-5

14. Jurkiewicz, P., Cwiklik, L., Jungwirth, P., Hof, M.: Lipid hydration and mobility: an interplay between fluorescence solvent relaxation experiments and molecular dynamics simulations. Biochimie **94**(1), 26–32 (2012). https://doi.org/10.1016/j.biochi.2011.06.027

15. Bagatolli, L.A.: LAURDAN fluorescence properties in membranes: a journey from the fluorometer to the microscope BT - fluorescent methods to study biological membranes. In: Mély, Y., Duportail, G. (eds), pp. 3–35. Springer, Heidelberg (2013)

16. Golfetto, O., Hinde, E., Gratton, E.: Laurdan fluorescence lifetime discriminates cholesterol content from changes in fluidity in living cell membranes. Biophys. J. **104**(6), 1238–1247 (2013). https://doi.org/10.1016/j.bpj.2012.12.057

17. Malacrida, L., Jameson, D.M., Gratton, E.: A multidimensional phasor approach reveals LAURDAN photophysics in NIH-3T3 cell membranes. Sci. Rep. **7**(1), 1–11 (2017). https://doi.org/10.1038/s41598-017-08564-z